Outer Sphere Electroreduction of CCl_4 in 1-Butyl-3-methylimmidazolium Tetrafluoroborate: An Example of Solvent Specific Effect of Ionic Liquid

Mohsin Ahmad Bhat,[†] Pravin P. Ingole, Vijay R. Chaudhari, and Santosh K. Haram*

Department of Chemistry, University of Pune, Ganeshkhind, Pune 411007, India

Received: November 4, 2008; Revised Manuscript Received: December 19, 2008

Electrodics of CCl_4 reduction in 1-butyl-3-methylimmidazolium tetrafluoroborate [BMIM][BF_4] room temperature ionic liquid (RTIL) is reported. A convolutive analysis of the cyclic voltammograms suggests that CCl_4 electroreduction follows stepwise (outer sphere) dissociative electron transfer pathway, rather than the sticky dissociative (inner sphere) electron transfer, as in the case of conventional organic solvents. This difference in the mechanism of electron transfer initiated bond cleavage is attributed to the solvent specific effects, namely, stabilization of $CCl_4^{\bullet -}$ intermediate radical anion in RTIL, which in turn decreases the electron transfer rate and thus the carbon−halogen bond cleavage rates. Electroreduction of CCl_4 in RTIL through outer sphere electron transfer would be a promising pathway for its direct conversion to methane.

1. Introduction

Owing to desired ionic conductivity and large electrochemical window, room temperature ionic liquids (RTILs) have received considerable attention as solvents/electrolytes for the electrochemical investigations and applications.[1−4] To date, most of the electrochemical studies in RTILs are related to their suitability as a "green" alternative to the conventional organic solvents.[5−7] It is presumed that the mechanism of electrochemical processes remains the same as that in conventional solvents—albeit with some effect on kinetic parameters, attributed to the difference in the physical properties of RTILs.[8−10]

Among various ionic liquids, dialkylimmidazolium-based RTILs (DAI-RTILs) are usually preferred in the electrochemical experiments[1,11,12] due to their appreciable conductivity and air and moisture stability. It is understood that DAI-RTILs form three-dimensional network of cations and anions and are viewed as nanostructured fluids.[13,14] The structural order in DAI-RTILs is envisaged to be responsible for the higher solvent reorganization, slower double layer interface relaxations, and hence slower electron transfer kinetics.[15] In addition, the possible interaction of electroanalyte or electrogenerated species with the constituent ions of RTIL[16] is also expected to influence the thermodynamic and kinetic aspects of electron transfer and electron transfer initiated processes.[1,17] In spite of these interesting possibilities, RTIL specific effects in electron transfer or electron transfer initiated processes have seldom been reported.[18−20] In this regard, electrochemical investigations of the solvent structure sensitive reactions, such as electron transfer initiated carbon−halogen (C−X) bond cleavage reactions,[21,23] seem to be a suitable choice to explore the solvent specific effects of RTILs. This reaction may proceed through any of following four different pathways, viz. (1) stepwise, (2) concerted, (3) sticky dissociative, and (4) almost dissociative electron transfer, as shown in the following scheme:[23]

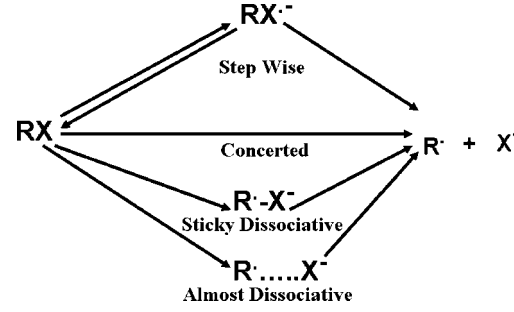

The most plausible mechanism depends on the stability of radical ion intermediate, electron transfer (k_{et}) and cleavage (k_c) rate constant of C−X bond, which are strongly influenced by the structure and extent of solvation. Among them, sticky dissociative (SDM) and almost dissociative (ADM) mechanisms represent an intermediate path between the stepwise and dissociative electron transfers and are strongly influenced by solvating capability of the solvent. Cyclic voltammetry has been proved to be very useful for the fundamental understanding and analytical investigations of their mechanistic details.[23−26]

One of the most studied systems is the electroreduction of CCl_4, which is demonstrated to follow SDM[25] in the organic solvents and very sensitive to the solvent characteristics.[26] To our knowledge, the mechanistic aspects of CCl_4 reduction in DAI-RTIL has not yet been studied so for. Therefore, it was chosen as a model reaction to understand solvent specific effect of [BMIM][BF_4]. It is worth emphasizing that the dechlorination of CCl_4 is a very important process for the groundwater purification, and RTILs have been proposed to be a suitable medium for the said process.[27] Therefore, the knowledge about the CCl_4 electroreduction in RTIL is expected to help in designing an efficient electrochemical dehalogenating setup for the halogenated pollutants.

Electrodics of CCl_4 reduction was therefore investigated with an aim to probe the role of [BMIM][BF_4] on the mechanistic aspect of its reduction. Chrono methods have been employed for the estimation of transport parameter, while cyclic voltammetry (CV) was used for the kinetic investigations. CV data were convoluted and analyzed in the light of various theories proposed for the electroreduction of alkyl halides in the conventional solvents.

* Corresponding author: e-mail haram@chem.unipune.ernet.in. Ph +91 20 2560 1394, Fax +91 20 2569 1728.

[†] Permanent address: Department of Chemistry, University of Kashmir, Srinagar 190006, India.

10.1021/jp809749k CCC: $40.75
Published on Web 02/06/2009

2. Experimental Section

Acetonitrile and ethyl acetate from Merck and 1-methylimmidazole, 1-chlorobutane, and tetrafluoroboric acid (40% aqueous solution) from Spectrochem, India, were procured. Ferrocene was purchased from Sigma-Aldrich and used after recrystallization from hexane. Carbon tetrachloride (Merck, India) was of spectra grade and used as received. Keeping in view the recommendations of Bond et al.,[4] "voltammetrically pure" [BMIM][BF_4] was synthesized using a reported method.[28] Gordon et al.'s recommendations[29] were considered for the purification of starting materials, conditions for quarternization, anion exchange reaction, and finally purification of RTILs. A detailed description about synthesis, characterization, and purification procedures is presented in the Supporting Information.

All electrochemical measurements were performed using Metrohm PGSTAT100 potentiostat/galvanostat in a three-electrode setup. A thermostated (±0.1 °C) and airtight jacket borosilicate cell having standard joints and provision to place the electrodes at a distance of ca. 5 mm from one other was designed for this purpose. Prior to the experiment, the cell was immersed in 2 M HNO_3 for 24 h, rinsed thoroughly with copious amount of Millipore water (ρ = 18 MΩ cm), and dried at 60 °C in an oven. Prior to use, [BMIM][BF_4] was vacuum-dried in a desiccator. All the measurements were carried out in the argon atmosphere. Ag wire (99.9%) and platinum (99.9%) loop were used as a quasi-reference and counter electrode, respectively. These were cleaned with dilute HNO_3 and then rinsed with a copious amount of Millipore water and vacuum-dried. A glassy carbon electrode (GCE) of geometric area 0.07 cm^2 was used as working electrode. It was gently polished over alumina powder (0.25 μm size), rinsed with a jet of Millipore water, and wiped with soft tissue paper soaked in ethanol. The effective area of the working electrode was determined through chronoamperometric measurements for the oxidation of ferrocene (10 mM), 0.1 M TBAP in acetonitrile. Using reported value of diffusion coefficient for ferrocene (2.3×10^{-5} cm^2 s^{-1}),[30] the roughness factor of the electrode was estimated to be ca. 1.1. Inbuilt positive feedback circuitry in the electrochemical workstation was used to evaluate and compensate the solution resistance. Electrochemical experiments were carried at relatively high concentrations of CCl_4 (10 mM) in view of expected low diffusion coefficients in a viscous medium of ionic liquids. All the CV data were background corrected prior to the analysis. The potential scale was callibrated by using ferrocene/ferrocenium couple as an internal probe. Convolution analysis was achieved using the algorithm suggested by Lawson and Maloy,[31] for which the codes were written in MATLAB. Numerical calculations and data fitting were performed through codes written in Origin 6.0 (Microcal Software Inc.).

3. Results and Discussion

Typical cyclic voltammogram (CV) recorded for 10 mM CCl_4 in [BMIM][BF_4] is shown in Figure 1 as trace a. Two cathodic peaks (C1 and C2) at −1.70 and −2.31 V, respectively, and an anodic peak (A1) at 0.65 V were observed. Subsequent addition of $CHCl_3$ in the same analyte led to the increase in height of cathodic peak (C2) as shown in Figure 1, trace b. This suggests the formation of $CHCl_3$, through reduction of CCl_4 at (C1), which is subsequently reduced at (C2). This two-step reduction of CCl_4 in [BMIM][BF_4] is similar to the one reported in DMF.[25] However, the anodic peak at A1 is not reported in DMF, and we attributed it to the oxidation of electrogenerated Cl^- formed in the cathodic processes at C1 and C2. Therefore, the overall

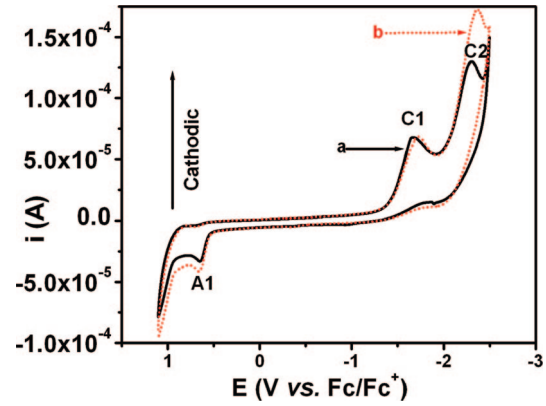

Figure 1. (a) Cyclic voltammogram recorded for 10 mM CCl_4 in [BMIM][BF_4] at 298 K on a GC electrode (scan rate 100 mV s^{-1}). Peak C1 corresponds to reduction of CCl_4, while peaks C2 and A1 correspond to reduction of electrogenerated $CHCl_3$ and oxidation of electrogenerated Cl^-, respectively. (b) CV recorded after addition of 10 μL of $CHCl_3$ in the same cell. Increase in peak height for peak C2 associates it to the reduction of $CHCl_3$, formed at C1.

redox process taking place in [BMIM][BF_4] can be schematically represented as

peak C1

$$CCl_4 + e^- \rightarrow Cl_3C^\bullet + Cl^- \quad (1)$$

$$Cl_3C^\bullet + e^- \rightarrow Cl_3C^- \quad (2)$$

$$Cl_3C^- + H^+ \rightarrow Cl_3CH \quad (3)$$

peak C2

$$Cl_3CH + e^- \rightarrow Cl_2CH^\bullet + Cl^- \quad (4)$$

$$Cl_2CH^\bullet + e^- \rightarrow Cl_2CH^- \quad (5)$$

peak A1

$$Cl^- - e^- \rightarrow \frac{1}{2}Cl_2 \quad (6)$$

Since, we were primarily interested in C−Cl bond cleavage in CCl_4, we restricted our detailed analysis to the process taking place at (C1), which corresponds to the reduction of CCl_4 in accordance with eqs 1 and 2.

Shift in the peak current (i_p) and peak potential (E_p) was observed as a function of scan rate ranging from 10 to 1000 mV s^{-1} (Figure S3, Supporting Information). A plot of i_p vs square root of scan rate ($\nu^{1/2}$) fits faithfully to a straight line (R^2 = 0.999) as shown in Figure 2a, while the peak potential shifts negatively with increase in scan rate as shown in Figure 2b. These features are associated with the diffusion-controlled irreversible electron transfer.[32] Figure 3 shows a plot of E_p vs log ν for peak C1, and from the slope, $\partial E_p/\partial \log \nu$ is found to be equal to 101 mV. Moreover, the value of $E_p - E_{p/2}$ is in the range 120−160 mV. Both these observations are associated with the electron transfer being the rate-determining step.[33]

The overall peak C1 has kinetic characteristics of a two-electron transfer. In first step, conversion of CCl_4 to $Cl_4C^{\bullet -}$ followed by its cleavage through either concerted or stepwise

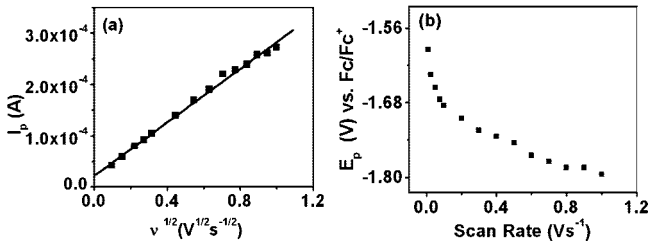

Figure 2. (a) Plot of i_p vs square root of scan rate for CCl_4 reduction at C1 on GC electrode in [BMIM][BF_4]. A solid line indicates the fit in the linear regression, suggesting a diffusion-controlled process. (b) Plot showing variation of peak potential with change in scan rate for peak C1 of Figure 1a.

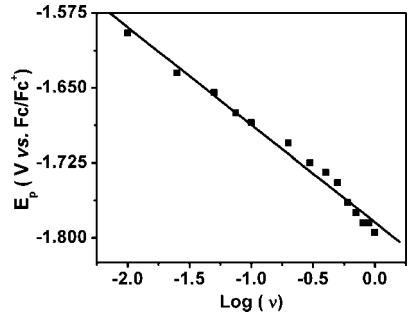

Figure 3. Peak potential vs log of scan rate (ν) for CCl_4 reduction on GC electrode in [BMIM][BF_4]. Data fit into the linear equation $E_p = -101\nu - 2.0026$. Slope of the linear regression indicates that the kinetics is controlled by electron transfer.

pathway to $Cl_3C^{\bullet}$ takes place. The second electron transfer leads to the subsequent reduction of $Cl_3C^{\bullet}$ to Cl_3C^{-}. Among these two reduction steps, the reduction of $Cl_3C^{\bullet}$ being more facile than that of the CCl_4 reduction, the conversion of CCl_4 to $Cl_4C^{\bullet -}$ is considered to be the rate-determining step.

To know the nature of the rate-determining step (stepwise or concerted) the electron transfer coefficient (α) was calculated from the peak width through

$$\alpha = \frac{1.86RT}{F|E_{p/2} - E_p|} \tag{7}$$

and the peak potential variation with scan rate through

$$\alpha = \frac{-RT}{F(\delta Ep/\delta \log \nu)} \tag{8}$$

Using this analysis, the estimated value of α was found to be in the range 0.27−0.38, which indicated prevalence of the concerted mechanism. Above conclusions are based on the conventional voltammetric analysis which uses a single or a pair of values characteristic to CV.[32,34,35] A much better and reliable approach in such situations would be the convolutive transformation of CV data, in which all the data points of voltammograms are used for the analysis. The convolutive analysis is also useful to determine the kinetic and thermodynamic parameters associated with the electron transfer process[23,25,36−39] and thus preferred in such cases. Forward scans of background-corrected CVs recorded at various scan rates were transformed by convolution of the current potential data into semi-integral current (I) vs potential curves, as per the following equation:[32,40]

$$I = \frac{1}{\pi}\int_0^t \frac{i_u}{\sqrt{(t-u)}}\,\mathrm{d}u \tag{9}$$

where i_u is the current at time u, prior to the time of evaluation (t) of I. The original peak-shaped curve as shown in Figure 4a gets transformed into a sigmoidal one as shown in Figure 4b. Here, the limiting value of the current (I_l) is proportional to the diffusion coefficient and concentration of electroanalyte. For the irreversible processes, the potential-dependent convoluted current ($I(E)$) obtained from CVs is related to the potential-dependent rate constant for electron transfer $k(E)$ through the equation[32]

$$\ln [k(E)] = \ln(\sqrt{D}) - \ln\left[\frac{I_l - I(E)}{i}\right] \tag{10}$$

with

$$I_l = nFAC^*\sqrt{D} \tag{11}$$

where A is the electrochemically active area of the electrode, D the diffusion coefficient of CCl_4, and C^* the bulk concentration. I_l was found to be almost independent of the scan rate. The value of the diffusion coefficient determined from I_l is equal to 1.42×10^{-6} $cm^2\ s^{-1}$ and is quite close within the experimental error limits to the value 1.60×10^{-6} $cm^2\ s^{-1}$, estimated through chronocoulometry (Figure S4, Supporting Information). These values are however an order of magnitude less than the one reported for the reduction of CCl_4 in DMF, perhaps on account of higher viscosity of [BMIM][BF_4]. $k(E)$ calculated from eq 10 as a function of applied electrode potential is shown in Figure 5a. From that, the potential-dependent electron transfer coefficient ($\alpha(E)$) values were calculated through

$$\alpha(E) = \left(-\frac{RT}{T}\right)\left[\frac{\partial \ln k(E)}{\partial E}\right] \tag{12}$$

These are not corrected for double-layer corrections; nevertheless, they are expected to be very close to the actual values on glassy carbon electrode.[25,26] $\alpha(E)$ obeys the relation

$$\alpha(E) = 0.5 + \left(\frac{F(E - E^\circ)}{8\Delta G_0^{\ddagger}}\right) \tag{13}$$

where E° is the formal potential and $\Delta G_0^{\ddagger}$ is the intrinsic barrier of the overall process. Values of α at all potentials in the whole range of the peak C1 were below 0.5, which is an indication of the dissociative electron transfer. The α (Figure S5, Supporting Information) fits in the linear relation

$$\alpha(E) = 0.307E + 0.758 \tag{14}$$

Equating eq 13 with eq 14 for the limit $E = E^\circ$ leads to the standard reduction potential for redox corresponding to peak C1 to be −0.84 V vs Fc/Fc^+. This value is almost 1 V less negative than the observed peak potentials and 0.2 V more negative than that reported in DMF.[25,26] Hence, both these differences emphasize that the concerted mechanism of electron transfer initiated C−X bond cleavage is operative for peak C1.

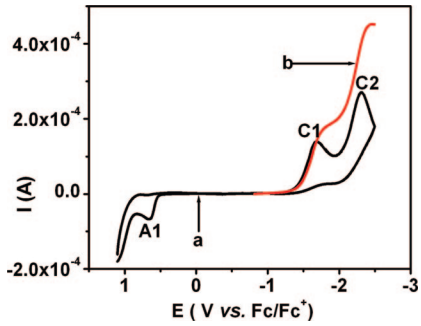

Figure 4. Convolutive transformation of CV recorded at 200 mV/s for 10 mM CCl_4 in [BMIM][BF_4]; trace a showing the original CV and trace b the corresponding convoluted form.

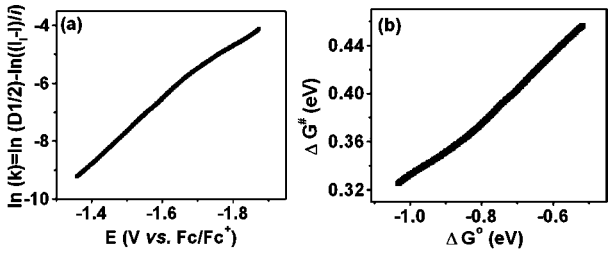

Figure 5. (a) Potential dependence of the ln $k(E)$ (heterogeneous electron transfer rate constant) for reduction of CCl_4 in [BMIM][BF_4] at 298 K; the plot is from convolutive analysis of the CV data. (b) Variation of the free energy of activation with the standard free energy of the reaction for the reduction of CCl_4 in [BMIM][BF_4].

To further pinpoint mechanistic aspects, the functional relation of potential-dependent free energy of activation ($\Delta G^{\ddagger}(E)$) with the electrode potential is estimated through

$$\Delta G^{\ddagger}(E) = \frac{RT}{F}\ln\left(\frac{Z}{k(E)}\right) \tag{15}$$

where $Z = (RT/2\pi M)^{1/2}$ ($= 5 \times 10^{-3}$ cm s^{-1}) and M is the molecular mass of the CCl_4. The extent of its dependence on applied potential (E) is very useful in determination of thermodynamic and kinetic parameters of the electron transfer process. $\Delta G^{\ddagger}(E)$ was calculated using eq 15, and the resulting values are plotted as a function of driving force ($E - E^{\circ}$) in Figure 5b. For the dissociative electron transfer process, $\Delta G^{\ddagger}(E)$ is expressed as

$$\Delta G^{\ddagger}(E) = \Delta G_0^{\ddagger}\left(1 + \frac{\Delta G^{\circ}}{4\Delta G_0^{\ddagger}}\right)^2 \tag{16}$$

where

$$\Delta G^{\circ} = F(E - E^{\circ}) \tag{17}$$

For the concerted pathway

$$\Delta G_0^{\ddagger} = \frac{\mathrm{BDE} + \lambda_0}{4} \tag{18}$$

and for stepwise pathway

$$\Delta G_0^{\ddagger} = \frac{\lambda_0}{4} \tag{19}$$

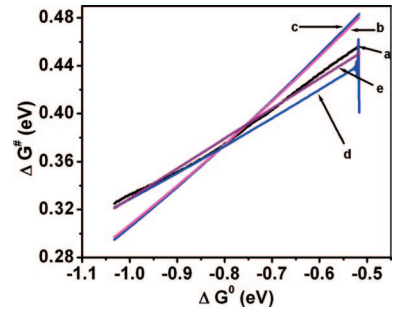

Figure 6. Variation of the free energy of activation with the standard free energy of the reaction for the reduction of CCl_4 in [BMIM][BF_4]: (a) experimental, (b) concerted dissociative electron transfer model, (c) sticky concerted dissociative electron transfer model with fixed solvent reorganization energy, (d) sticky concerted dissociative electron transfer model with solvent reorganization energy dependent on extent of bond cleavage, and (e) proposed stepwise outer sphere dissociative electron transfer model.

Here, BDE represents the bond dissociation energy of C−Cl bond and λ_0 the solvent reorganization energy. Recent reports[41,42] show that the solvent fluctuations associated with electrochemical redox processes in ionic liquids, like in conventional solvents, are quadratic as required by the Marcus theory. In light of these reports, which justify the use of continum model for short chain dialkylimidazolium-based RTILs, λ_0 was calculated through

$$\lambda_0 = \frac{e}{8\pi\epsilon_0 a_0}\left[\frac{1}{\epsilon_{\mathrm{opt}}} - \frac{1}{\epsilon_{\mathrm{stat}}}\right] \tag{20}$$

where ϵ_{stat} and ϵ_{opt} are the static and optical dielectric constants of the solvent and assume the values 11.7[43] and 2.0[44] for [BMIM][BF_4], respectively. a_0 is the effective radius of CCl_4 and is calculated through

$$a_0 = a_{\mathrm{Cl}}\left[\frac{2a_{\mathrm{CCl_4}} - a_{\mathrm{Cl}}}{a_{\mathrm{CCl_4}}}\right] \tag{21}$$

λ_0 is calculated by using $a_{\mathrm{Cl}} = 1.81$ Å and $a_{\mathrm{CCl_4}} = 3.71$ Å.[25] Plugging the values of λ_0 and BDE for C−Cl in CCl_4 (2.84 eV), the intrinsic barrier was expected to be equal to ca. 1.0 and 0.3 eV for concerted and stepwise mechanisms, respectively.

$\Delta G^{\ddagger}(E)$ values calculated as per the above equations were found to vary significantly from the experimental values as shown in Figure 6. The optimized match between the two sets of values was observed at the intrinsic barrier of ca. 0.72 eV, which is lower than expected for truly concerted and at the same time much higher than expected for truly stepwise mechanisms. This type of mismatch between the theoretical and experimental values has been previously explained on the basis of radical−ion pair interaction for electroreduction in the case of CCl_4,[25] haloacetonitriles,[36] and polychloroacetamides.[45] The mechanism in such cases is regarded as a special case of dissociative electron transfer and termed as sticky dissociative electron transfer. According to this, $\Delta G^{\ddagger}(E)$ is strongly influenced by possible interaction between the radical and the anion, formed on account of concerted dissociative electron transfer. In such cases, $\Delta G^{\ddagger}(E)$ is given by

$$\Delta G^{\ddagger} = \Delta G_0^{\ddagger}\left(1 + \frac{\Delta G^{\circ} - D_p}{4\Delta G_0^{\ddagger}}\right)^2 \quad (22)$$

and

$$\Delta G_0^{\ddagger} = \frac{(\sqrt{\mathrm{BDE}} - \sqrt{D_p})^2 + \lambda_0}{4} \quad (23)$$

Here, D_p represents strongly solvent-dependent ion−radical interaction among dissociated products. When this model was used for the calculation of $\Delta G^{\ddagger}(E)$, the theoretical values did not match significantly with the experimental ones, even with high values of radical−ion interaction energies. Therefore, we tried an advanced version of this model, where the solvent reorganization energy is assumed to vary with the extent of bond breakage and as per this[25,36,46]

$$\Delta G^{\ddagger}(E) = \mathrm{BDE}\cdot Y^{\ddagger 2} + [\lambda_0^{\mathrm{R}} + (\lambda_0^{\mathrm{P}} - \lambda_0^{\mathrm{R}})Y^{\ddagger}]X^{\ddagger 2} \quad (24)$$

$$Y^{\ddagger} = \left(1 - \sqrt{\frac{D_p}{\mathrm{BDE}}}\right)X^{\ddagger} - \frac{\lambda_0^{\mathrm{P}} - \lambda_0^{\mathrm{R}}}{2\mathrm{BDE}}X^{\ddagger}(1 - X^{\ddagger}) \quad (25)$$

$$\Delta G_0^{\ddagger} = D_p + \mathrm{BDE}\left[1 - \sqrt{\frac{D_p}{\mathrm{BDE}}}\right]\left[2Y^{\ddagger} - \left(1 - \sqrt{\frac{D_p}{\mathrm{BDE}}}\right)\right] + [\lambda_0^{\mathrm{R}} + (\lambda_0^{\mathrm{P}} - \lambda_0^{\mathrm{R}})Y^{\ddagger}](2X^{\ddagger} - 1) \quad (26)$$

With this model, even with high values such as 250 meV for D_p, significant mismatch between the theoretical and experimental values was observed, which becomes more prominent upon increase in driving force of the reaction, as shown in Figure 6.

With the help of ab initio calculations,[47] it has been proved that the trajectories connecting valleys of products and reactants in the potential energy surface for reduction of CCl_4 to $CCl_3^{\bullet}$ and Cl^- do have two minima corresponding to compressed and elongated geometries of the intermediate $CCl_4^{\bullet -}$. So, we model the rate-determining step corresponding to electroreduction at peak C1 as a stepwise process, with an intrinsic barrier given by

$$\Delta G_0^{\ddagger}(\mathrm{stepwise}) = \frac{\lambda_0 + P}{4} \quad (27)$$

where P is a measure of internal reorganization energy associated with the formation of $CCl_4^{\bullet -}$ from CCl_4. It may be equal to vertical or adiabatic electron affinity depending upon the nature of $CCl_4^{\bullet -}$ formed. As per the above model, with P as an adjustable parameter and λ_0 as calculated from eq 20, a best fit between the experimental and theoretical values ($R^2 = 0.999$) for $\Delta G^{\ddagger}(E)$ (Figure 6) is achieved with $P = 1.1$ eV. The said value of P matches very well to the adiabatic electron affinity reported for CCl_4.[48] A comparative account of the predicted $\Delta G^{\ddagger}(E)$ from various proposed models, and our model is shown in Figure 6. Though the magnitude of $\alpha(E)$ obtained from $\Delta G^{\ddagger}(E)$ indicates the concerted dissociative electron transfer, the experimentally observed values for $\Delta G^{\ddagger}(E)$ did not get along with the models for concerted dissociative electron transfer (inner sphere model: dissociative, sticky dissociative, almost dissociative). Instead, the values fit in model based on stepwise electron transfer initiated C−X bond cleavage (outer sphere model), associated with a significant extent of internal reorganization energy. Transition of mechanism from inner sphere to outer sphere one, in electroreduction of CCl_4, through solvent specific effects was predicted by Zhang et al.[48] through ab initio methods. We also attribute this change in the mechanism of electroreduction of CCl_4 to solvent specific effects of RTIL. A careful analysis of these electron transfers shows that the overall observed mechanism is an outcome of kinetic and thermodynamic aspects of two steps: (a) electron transfer to the analyte to form radical anion and (b) cleavage of C−X bond in radical anion to form C-centered radical and X^-, characterized by rate constants k_{et} and k_c, respectively, as follows:

$$CCl_4 + e^- \xrightarrow{k_{et}} {}^-Cl{-}Cl_3C^{\bullet} \quad (28)$$

$${}^-Cl{-}Cl_3C^{\bullet} \xrightarrow{k_c} Cl_3C^{\bullet} + Cl^- \quad (29)$$

A high value of k_c implies fast cleavage of the C−X bond and supports concerted dissociative electron transfer, and a low value of k_c implies the stepwise mechanism. Theoretical calculations for the formation of $CCl_4^{\bullet -}$ [47] indicated a vertical attachment of electron to the CCl_4, followed by change in geometrical parameters through spin and electron dynamics, involving the energy redistribution. The corresponding contour plots show that the electron is initially localized on central C atom and charge spread over an entire molecule. On a picosecond time scale, C−Cl bond cleavage takes place through changes in the electron and spin density distribution associated with changes in the geometrical parameters. Stabilization of $CCl_4^{\bullet -}$ through interaction of RTIL cation and diffuse electron cloud of radical anion is expected to slow down the electrodynamic process of negative charge transfer from C-centered sp^3 orbital to the p orbital of leaving Cl^- ion and hence lowering the value of k_{et}. The reasoning seems true in light of recent electrochemical[19,20] and pulse radiolysis[50] reports, which indicated significant stabilization of electrogenerated radical anions by dialkylimmidazolium cations. High molecular organization prevalent in RTILs is expected to have high values of λ_0 associated with C−Cl bond cleavage in $CCl_4^{\bullet -}$ and hence lowering the k_c. Slow electron transfer kinetics in RTILs (low k_{et}) implies higher energy of electron for reduction process, which also favors stabilization of $CCl_4^{\bullet -}$ by increasing gap between transition state and $CCl_4^{\bullet -}$ minima.[48] Perhaps, the present case is an example of electron transfer, concerted with the ion pairing followed by the bond breaking. The ion pairing is responsible for the kinetic cost, viz. high reorganization energy and hence more negative potentials for the CCl_4 reduction. On the other hand, it has a thermodynamic advantage in terms of lowering the energy of intermediates.[49]

Thus, we propose that outer sphere mechanism for electroreduction of CCl_4 in [BMIM][BF_4] is on account of low k_c and k_{et} values due to structural features of the RTIL and the electrostatic interactions. Both these features are responsible for stabilization and temporary existence of $CCl_4^{\bullet -}$ as an intermediate. Formation of matrix-stabilized $CCl_4^{\bullet -}$ has been earlier experimentally demonstrated by Bonazzalo et al.[51] The values of α lower than 0.5 for this electroreduction (which indicates dissociative electron transfer) may be one of the cases of

stepwise mechanisms, where the slow heterogeneous electron transfer in electrochemically irreversible processes pushes the peak potential negatively and leads to α values less than 0.5, though the mechanism is stepwise.[39] This is expected for stepwise dissociative electron transfers in RTILs as the electron transfer kinetics has been demonstrated to be very slow.[1,9,19,50] Studies related to low α values for stepwise mechanism in the investigated RTIL are under way.

4. Conclusion

Electrodics of CCl_4 reduction in [BMIM][BF_4] has been investigated. Analysis of convoluted cyclic voltammetric data in light of various proposed theories for halocarbon reduction proves that the CCl_4 reduction in the ionic liquid occurs through stepwise pathway and not as per the concerted pathway that it has been demonstrated to follow in conventional solvents. The change in mechanism is attributed to solvent specific effect of [BMIM][BF_4], especially stabilization of $CCl_4^{\bullet -}$ due to its interaction with $[BMIM]^+$ cation. The said mechanism is supposed to be very advantageous for direct electrochemical conversion of environmentally poisonous halocarbons to their hydrocarbon analogues.

Acknowledgment. The authors dedicate this work to the memory of late Prof. S. K. Rangarajan (formerly Professor, Department of Inorganic and Physical Chemistry, Indian Institute of Science (IISc), Banglore, India), who expired on 29th, April 2008, barely 5 months after he taught us how to do convolution analysis of the CV data. We also thank Dr. Vijayamohanan K. Pillai (NCL, India) for the helpful discussions on several points. M.A.B. thanks University authorities—especially Vice Chancellor, University of Kashmir, and Head, Department of Chemistry, University of Kashmir—for sanction of study leave in his favor. P.P.I. thanks CSIR, India, for the fellowship. V.R.C. thanks BARC-Pune university collaborative Ph.D. program for financial support. The authors also thank CNQS, University of Pune, for financial support.

Supporting Information Available: A detailed procedure for synthesis and purification of [BMIM][BF_4]; ^{1}H NMR spectra of 1-butyl-3-methylimmidazolium chloride, [BMIM][Cl], and 1-butyl-3-methylimmidazolium hexafluorophosphate, [BMIM]-[BF_4]; cyclic voltammograms recorded at varying scan rates; Cotrell plot for chronocoulometric response to reduction of CCl_4 in [BMIM][BF_4]; and a plot showing variation of α with potential for reduction of CCl_4 in [BMIM][BF_4]. This material is available free of charge via the Internet at http://pubs.acs.org.

References and Notes

(1) Hapiot, P.; Lagrost, C. *Chem. Rev.* **2008**, *108*, 2238.
(2) *Electrochemical Aspects of Ionic Liquids*; Ohno, H., Ed.; John Wiley and Sons: Hoboken, NJ, 2005.
(3) Welton, T. *Chem. Rev.* **1999**, *99*, 2071.
(4) Zhang, J.; Bond, A. M. *Analyst* **2005**, *130*, 113.
(5) Fuller, J.; Carlin, R. T.; Osteryoung, R. A. *J. Electrochem. Soc.* **1997**, *144*, 3881.
(6) Boxall, D. L.; O'Dea, J. J.; Osteryoung, R. A. *J. Electrochem. Soc.* **2002**, *E468*.
(7) Hultgren, V. M.; Mariotti, A. W. A.; Bond, A. M.; Wedd, A. G. *Anal. Chem.* **2002**, *74*, 3151.
(8) Lagrost, C.; Preda, L.; Volanschi, E.; Hapiot, P. *J. Electroanal. Chem.* **2005**, *585*, 1.
(9) Quinn, B. M.; Ding, Z.; Moulton, R.; Bard, A. J. *Langmuir* **2002**, *18*, 1734.
(10) Lagrost, C.; Carrie, D.; Vaultier, M.; Hapiot, P. *J. Phys. Chem. A* **2003**, *107*, 745.
(11) dupont, J.; Suarez, P. A. Z. *Phys. Chem. Chem. Phys.* **2006**, *8*, 2441.
(12) Endres, F.; Abedin, S. Z. E. *Phys. Chem. Chem. Phys.* **2006**, *8*, 2101.
(13) Canongia Lopes, J. N.; Padua, A. A. H. *J. Phys. Chem. B* **2006**, *110*, 3330.
(14) Xiao, D.; Rajian, J. R.; Cady, A.; Li, S.; Bartsch, R. A.; Quitevis, E. L. *J. Phys. Chem. B* **2007**, *111*, 4669.
(15) Brooks, C. A.; Doherty, A. P. *J. Phys. Chem. B* **2005**, *109*, 6276.
(16) Hydrogen bonding, electrostatic or van der Waals interactions, $\pi-\pi$ and $n-\pi$ stacking.
(17) Anderson, J. L.; Ding, J.; Welton, T.; Armstrong, D. W. *J. Am. Chem. Soc.* **2002**, *124*, 14247.
(18) Lagrost, C.; Hapiot, P.; Vaultier, M. *Green Chem.* **2005**, *7*, 468.
(19) Lagrost, C.; Gmouh, S.; Vaultier, M.; Hapiot, P. *J. Phys. Chem. A* **2004**, *108*, 6175.
(20) Zigah, D.; Ghilane, J.; Lagrost, C.; Hapiot, P. *J. Phys. Chem. A* **2008**, ASAP.
(21) Saveant, J.-M. *Acc. Chem. Res.* **1978**, *109*, 6787.
(22) Costentin, C.; Robert, M.; Saveant, J.-M. *Chem. Phys.* **2006**, *324*, 40.
(23) Houmam, A. *Chem. Rev.* **2008**, *108*, 2180.
(24) Bhat, M. A.; Ingole, P. P.; Chaudhari, V. R.; Haram, S. K. *New J. Chem.* **2009**, *33*, 207.
(25) Pause, L.; Robert, M.; Saveant, J.-M. *J. Am. Chem. Soc.* **2000**, *122*, 9829.
(26) Prasad, M. A.; Sangaranarayanan, M. V. *J. Electroanal. Chem.* **2004**, *569*, 127.
(27) Barhdadi, R.; Courtinard, C.; Nedelec, J. Y.; Troupel, M. *Chem. Commun.* **2003**, 1434.
(28) Dupont, J.; Consorti, C. S.; Suarez, P. A. Z.; de Souza, R. F. *Org. Synth.* **1999**, *79*, 236.
(29) Gordon, C. M.; Maclean, A. J.; Muldoon, M. J.; Dunkin, R. I. In *Ionic Liquids as Green Solvents: Progress and Prospects*; Rogers, R. D., Seddon, K. R., Eds.; ACS Symposium Series 856; American Chemical Society: Washington, DC, 2003.
(30) Marsh, K. N.; Deev, A.; Wu, A. C.-T.; Tran, E.; Klamt, A. Kor. *J. Chem. Eng.* **2002**, *19*, 357.
(31) Lawson, R. J.; Maloy, T. *Anal. Chem.* **1974**, *46*, 559.
(32) Bard, A. J.; Faulkner, L. R. *Electrochemical Methods. Fundamentals and Applications*, 2nd ed.; John Wiley and Sons: New York, 2001.
(33) (a) Nadjo, L.; Saveant, J.-M. *J. Electroanal. Chem.* **1973**, *48*, 113. (b) Andrieux, C. P.; Saveant, J.-M. Electrochemical Reactions. In *Investigations of Rates and Mechanisms of Reactions*; Bernasconi, C. F., Ed.; Wiley and Sons: New York, 1986; Vol. VI/4E, Part 2, pp 305−390.
(34) Nicholson, R. S.; Shain, I. *Anal. Chem.* **1964**, *36*, 706.
(35) Nadjo, L.; Saveant, J.-M. *J. Electroanal. Chem.* **1973**, *48*, 113.
(36) Cardinale, A.; Isse, A. A.; Gennaro, A.; Robert, M.; Saveant, J.-M. *J. Am. Chem. Soc.* **2002**, *124*, 13533.
(37) Antonello, S.; Maran, F. *J. Am. Chem. Soc.* **1997**, *119*, 12595.
(38) Donkers, R. L.; Workentin, M. S. *J. Phys. Chem. B* **1998**, *102*, 4061.
(39) Antonello, S.; Maran, F. *J. Am. Chem. Soc.* **1999**, *121*, 9668.
(40) Imbeaux, J. C.; Saveant, J.-M. *J. Electroanal. Chem.* **1973**, *44*, 169.
(41) Shim, Y.; Kim, H. J. *J. Phys. Chem. B* **2007**, *111*, 4510.
(42) Lynden-Bell, R. M. *J. Phys. Chem. B* **2007**, *111*, 10800.
(43) Wakai, C.; Oleinikova, A.; Ott, M.; Weinga1rtner, H. *J. Phys. Chem. B* **2005**, *109*, 17208.
(44) Koeberg, M.; Wu, B. C.-C.; Kim, C. D.; Bonn, M. *Chem. Phys. Lett.* **2007**, *439*, 60.
(45) Costentin, C.; Louault, C.; Robert, M.; Teillout, A.-E. *J. Phys. Chem. A* **2005**, *109*, 2984.
(46) Pause, L.; Robert, M.; Saveant, J.-M. *J. Am. Chem. Soc.* **2001**, *123*, 11908.
(47) Tachikawa, H. *J. Phys. Chem. A* **1997**, *101*, 7454.
(48) Zhang, N.; Blowers, P.; Farrell, J. *Environ. Sci. Technol.* **2005**, *39*, 612.
(49) Saveant, J.-M. *J. Am. Chem. Soc.* **2008**, *130*, 4732.
(50) (a) Behar, D.; Gonzalez, C.; Neta, P. *J. Phys. Chem. A* **2001**, *105*, 7607. (b) Behar, D.; Neta, P.; Schultheisz, C. *J. Phys. Chem. A* **2002**, *106*, 3139. (c) Grodkowski, J.; Neta, P. *J. Phys. Chem. A* **2002**, *106*, 5468. (d) Grodkowski, J.; Neta, P. *J. Phys. Chem. A* **2002**, *106*, 9030. (e) Grodkowski, J.; Neta, P. *J. Phys. Chem. A* **2002**, *106*, 11130. (f) Grodkowski, J.; Neta, P.; Wishart, J. F. *J. Phys. Chem. A* **2003**, *107*, 9794.
(51) Bonazzola, L.; Michaut, J. P.; Ronein, J. *Chem. Phys. Lett.* **1988**, *153*, 52.

JP809749K